Journal of Corrosion and Materials
www.corromat.com

J. Corros. Mater. (2026) 5(1), 36–49.

Extrusion-Printed GelMA/HAMA Lattices with Covalently Anchored QHREDGS for Vascularized Full-Thickness Wound Repair

Manfred T. Reetz[1,*]

Max Planck Institute for Coal Research, Kaiser-Wilhelm-Platz 1, 45470 Mülheim an der Ruhr, Germany

*Corresponding author: reetz@mpi-muelheim.mpg.de

(Received: 30 January 2026. Received in revised form: 10 April 2026. Accepted: 28 April 2026. Published online: 30 June 2026.)

Abstract

Porosity in hydrogel dressings can enhance tissue contacts and fluid exchanges, although the same property that enables effective transport may also expedite bioactive molecule depletion. This work investigates whether covalent immobilization of an angiopoietin-1-derived peptide sequence QHREDGS can keep an angiogenic signal within a GelMA/HAMA wound patch with structural characteristics and degradability necessary for skin regeneration. A photocrosslinkable mixture of 15% (w/v) GelMA, 5% (w/v) HAMA, 1% (w/v) HMPP, and 2% sodium alginate was extruded into circular lattices with a diameter of about 15 mm, cured by UV illumination at 365 nm and 10 mW cm^{-2} for 5 min, and modified by the EDC/NHS-based coupling of QHREDGS. Mechanical behavior, lattice structure, degradation rate, FITC-peptide retention, cytocompatibility, scratch and tube formation assays, and hemolytic testing of the material were performed, as well as in vivo tests using a rat full-thickness wound model. The printed structure had an open porous architecture, spongy inner structure and degraded by approximately 51.4% in 2 U mL^{-1} collagenase II within seven days. Fluorescent labeling confirmed quick peptide disappearance from physical adsorption, especially in thin filaments, and the significantly higher retention of the covalently anchored peptides throughout the entire observation period. Both the extract from the printed hydrogel and that from the hydrogel with coupled peptides demonstrated high cytocompatibility and the latter increased migration of fibroblasts and tube formation of human umbilical vein endothelial cells. Wound patch treatment with the covalent peptide-functionalized lattice resulted in the fastest wound healing, the best regenerated tissue development, less IL-6 and TNF-α staining, stronger collagen deposition, and the highest CD31/α-SMA-positive vascular density. The results obtained provide evidence that the therapeutic effect is not due to the presence of hydrogel itself but to its combined properties such as porosity, degradability and angiogenic signal delivery.

Keywords: GelMA; HAMA; QHREDGS; peptide immobilization; printed hydrogel; angiogenesis; collagenase degradation; wound healing; tissue repair.

1. Introduction

Skin restoration involves the coordinated series of biological events that take place rather than the surface contraction itself [1]. In order to heal, the wound should change from clot formation, inflammatory cells recruitment to fibroblast migration, vascular invasion, provision of the provisional tissues, resurfacing of the epithelium, and finally remodeling [2]. Each step failure might result in the delay in closure or creation of weak scar tissues. The biology of the process is highly dependent on the presence of inflammation and oxygen. The inflammatory mediators play essential roles in the early stages of injury; however, the transition of inflammation to proliferation is needed in order to successfully finish healing [3]. The persistence of IL-6, TNF-α, proteolytic enzymes, and hypoxic stress inhibits the functions of fibroblasts and vascular organization [4]. The dressings applied to the wound, therefore, should be assessed not only by their ability to reduce the wounded area [5]. They have to be capable of providing hydration and protection, exchange with the wound tissue, the absence of cytotoxic substances and biological cues for the initiation of tissue reconstruction [6]. Chronic wounds represent one more example of why biological regulation of the wound interface is important [7].

Hydrogels are widely studied for wound application due to the fact that their water-filled polymer network has some physical similarities with hydrated soft tissues and can be used as drug depots, tissue scaffolds, or temporary barriers [8]. However, their biological potential is controlled by the structural and temporal dynamics. Dense hydrogels will cover the defect well but they will limit the exudate exchange and the cellular access. Porous hydrogels will provide the exchange capability but can lose loaded drugs very quickly due to their high degradation rate in the proteolytic environment of the wound [14]. Therefore, the printed wound contact hydrogel should solve three problems at once: it has to be able to maintain its form after being placed, degrade enough to provide room for tissue replacement, and maintain the biological signals during the period of their effectiveness. These requirements are interdependent. Increased porosity provides better exchange capabilities and decreases the retention; increased crosslinking provides better retention and slows down remodeling. The engineering challenge, thus, is to find the balance between exchange, degradation, and signal persistence.

Gelatin methacryloyl represents good basis for such a balance due to the combination of gelatin-like chemistry and photocrosslinkable methacryloyl groups [9]. GelMA is also a source of the cell-interactive microengineered hydrogel [10]. It is possible to create the hydrogel network using the light-induced process and the gelatin network will be still available for the enzymatic remodeling [11].

Hyaluronic acid methacryloyl represents the second component of the network which is similar to the hydrated glycosaminoglycan phase [12]. Therefore, the blend of GelMA and HAMA is promising due to the fact that GelMA provides the cell-adhesive and degradable protein chemistry, while HAMA provides the hydrated glycosaminoglycan-like phase [13]. In order to use this blend for wound treatment, it is also necessary to print the material since a randomly distributed gel will not provide the control over the fluid exchange through the material. Extrusion printing can be used to create a hydrogel lattice of defined patch diameter, filament width, and open interfilament channels [14]. Such kind of the structure is particularly useful for the skin regeneration due to the ability of the lattice to cover the defect but not to behave like a continuous film [15].

The geometrical advantage of the printed lattice represents the main weakness of this structure that is being studied here. Large interfilament channels and thin filaments increase the surface for exchange but also reduce the diffusion length of the peptide or other signals. The molecules absorbed by the hydrogel can disappear before the wound reaches the phase when the sprouting of the new blood vessels and collagen production become efficient. This property is especially critical for the pro-angiogenic cues. The vascularization is responsible for supplying oxygen, nutrients, inflammatory cells, pericyte interaction, and paracrine signals that organize the collagen [16]. Tissue-engineered construct should not only support the endothelial networks but also provide vascular organization [17]. Therefore, the therapeutic angiogenic material should provide the control over the localization, accessibility, and residence of the signals [18]. The delivery of the exogenous growth factors can be used to promote angiogenesis as it was shown by the works on the bioartificial matrices for therapeutic vascularization [19]. However, the use of growth factor systems is limited due to the short residence time, instability, dose sensitivity, and the need for conjugation strategies [20]. Peptides can provide an alternative since they are chemically defined and can be used for the conjugation [21]. Modern peptide chemistry allows controlling the presentation of the peptide in the network [22].

QHREDGS is the peptide derived from the angiopoietin-1 that increases the endothelial survival, metabolism, and tube formation [23]. This peptide has been demonstrated to be cytoprotective in the human-cell culture systems [24]. Due to the size and chemical characteristics, it can be used as a test ligand in order to determine the possibility of the maintenance of the angiogenic signal in the printed lattice. The problem is not only whether the hydrogel will be able to contain the peptide at the moment of fabrication. It is important whether the peptide will be maintained in the material after its hydration, diffusion, and remodeling. The printed lattice will not be bioactive in case it will not be possible to link the peptide chemistry, lattice geometry, degradation, and biological effect in the same evidence chain.

Therefore, this research investigates the possibility to retain the bioactivity of the peptide covalently attached to the printed hydrogel matrix based on the GelMA/HAMA blend. The question is tested on the level of material, cellular, and tissue scales. The material-related evidence includes the morphology of the lattice, the porosity observed via SEM, collagenase II degradation, and FITC-peptide retention in thin and thick filaments. The cellular evidence includes the viability, migration of human dermal fibroblasts and the human umbilical vein endothelial cell tube formation. The tissue-related evidence includes wound closure, thickness of the regenerate, IL-6 and TNF-α staining, collagen deposition, and CD31/α-SMA immunofluorescence.

The broader literature shows why the research question presented here cannot be reduced to a choice between the natural and synthetic wound dressings. In classical wound-healing studies, it was shown that the wound closure depends on the processes of formation of the provisional tissues, fibroblast invasion, angiogenesis, and remodeling rather than on the surface coverage [25]. The transitions between these processes are regulated by the growth factors and cytokines [26]. The engineered skin therefore needs both the protective structure and biologically supporting interface [27]. Data about clinical outcomes and costs also emphasize the importance of the wound care strategy that improves repair rather than coverage [28]. The hydrogel studies come to the same conclusions on the materials level: scaffold performance is based on the balance between the structure, transport, and degradation [29]. The cell compatibility should be taken into account even when the network is chemically modified [30]. The porosity and microarchitecture are also important due to the exchange, cellular access, and remodeling [31]. The lines of evidence intersect in the wound interface. Biologically inert material will be useful in protecting the defect but cannot guide the vascularized repair, while the soluble cue without the retention mechanism will diffuse away before the fibroblasts and endothelial cells organize. Thus, the GelMA/HAMA-QHREDGS patch combines three key elements: the geometry allowing the exchange, the degradable network, and the covalent attachment of the peptide.

The angiogenic focus is important because the blood vessel formation is not the late isolated endpoint. Angiogenesis is connected with the inflammation, fibroblast functions, and collagen deposition. The endothelial invasion is induced by the hypoxia and the gradient of cytokines, but formed vessels have to be organized enough to support the tissue repair and not the transient sprouting [32]. In the biomaterials field, the most effective pro-angiogenic system is not the one with the highest ligand dose. Presentation, network degradability, cellular access, and signal exposure time play important role in the response [18]. QHREDGS was chosen for its potential since this short angiopoietin-derived peptide can be attached to the hydrogel and demonstrates endothelial activity [23]. Therefore, the material-related question is whether this immobilized ligand can remain active in the open printed hydrogel during the same interval in which the neovascularization and collagen deposition occur.

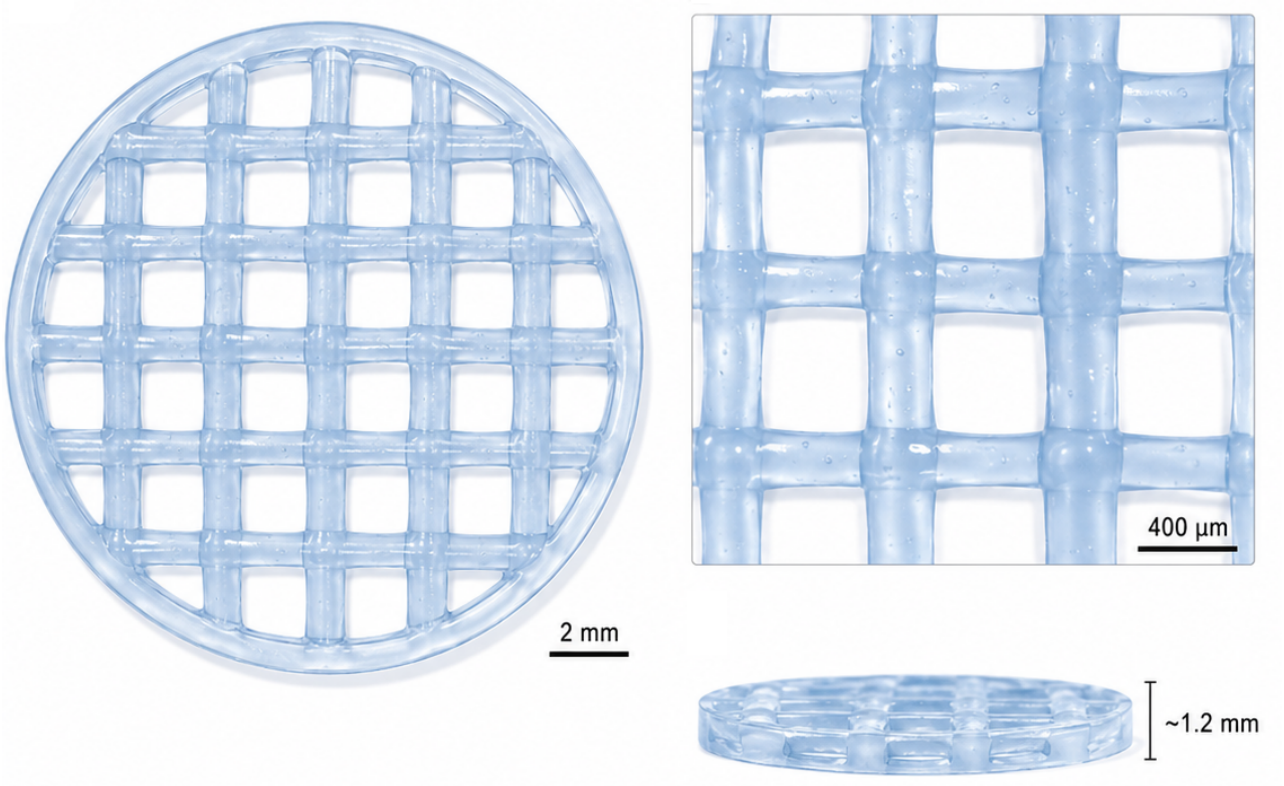

Figure 1: Printed lattice and fabrication details.

The material perspective in Fig. 1 describes the precise construct that will be studied. Specifically, the circular GelMA/HAMA lattice, enlarged filament structure, side view, formulation, conditions for UV exposure, and QHREDGS coupling via EDC/NHS chemistry is shown as the physical substrate for all further assays. Consequently, QHREDGS will not be considered as a freely dissolved additive upon its addition; it will be described as a material-linked ligand attached to a printed and photocrosslinked wound contact patch. Later comparisons to treatment with a patch and free peptide will reveal whether a locally linked ligand affects cell response and healing.

2. Materials and Methods

QHREDGS peptide and FITC-labeled QHREDGS peptide were purchased from Hefei Synthbio Co., Ltd. GelMA and HAMA were purchased from Engineering for Life Co., Ltd. Human dermal fibroblasts and human umbilical vein endothelial cells were purchased from Cyagen Biosciences. Fetal bovine serum and F12/Dulbecco's modified Eagle's medium were purchased from HyClone. Calcein-AM/PI staining kit was purchased from Invitrogen, growth factor-reduced Matrigel from BD Bioscience, collagenase II from Sigma-Aldrich, and CCK-8 reagent from Keygen Biotech Co. Male Sprague-Dawley rats aged 6-8 weeks were purchased from Hunan SJA Laboratory Animal Co., Ltd. All experimental procedures performed on animals met the Animal Ethics Committee guidelines of Jiujiang University.

The hydrogel ink for printing was prepared by dissolving 15% (w/v) GelMA, 5% (w/v) HAMA, and 1% (w/v) 2-hydroxy-2-methylpropiophenone in 2% sodium alginate solution. The well-known methodology of GelMA fabrication proves photocrosslinking as an effective method of producing gelatin-based hydrogels [33]. Ink was loaded into 5 mL syringe with flat-tip 20G and 23G needles of approximately 600 μm and 300 μm inner diameter respectively, and was printed by means of modified 3D-printer. HAMA-containing bioink has also been developed in order to provide printability and hydration [34]. Circular lattices of approximately 15 mm diameter were fabricated using these printing conditions. The temperature in the dispenser was set at 30 °C, and in the printing bed – at 10 °C to provide stability of filaments. Both parameters are needed to ensure extrusion and post-deposition stability of bioink [35]. Upon deposition, the constructed hydrogel lattices were photocrosslinked under 365 nm ultraviolet light at 10 mW cm^{-2} for 5 min.

The morphology of the material was studied by means of photography, optical microscopy, and scanning electron microscopy. Optical images helped to estimate the circular shape of a patch and its lattice precision, whereas scanning electron microscopy helped to assess the surface and internal porous structure. To prepare samples for SEM, they were freeze-dried for 24 h at -55 °C and 6.5 hPa, gold-sputtered, and visualized. It is crucial to evaluate both optical and SEM images as the first image describes the wound-scale pathway of the exchange, whereas the second one reveals the freeze-dried internal microstructure, which influences hydration, enzyme access and cell-material interactions.

Enzymatic degradation of the materials was estimated in collagenase II solution in order to simulate protease activity near the remodeling wound site. Freeze-dried samples were weighted beforehand and designated as W_0. Samples were incubated in 2 U

mL^{-1} collagenase II solution in PBS at 37 °C, and solution was changed daily. After specified time periods, samples were collected, freeze-dried again, and weighed as W_t. The remained dry weight was calculated as

$$W_D(\%) = \frac{W_t}{W_0} \times 100. \tag{1}$$

It is important to note that the formula above calculates the remaining material rather than degraded. This is important since the wound patch must not degrade as quickly as possible. It should be durable enough to cover the wound and deliver bioactive cues to wound tissue, but must degrade as much as needed for replacement by native dermis.

Peptide coupling was performed by EDC/NHS chemistry. Printed GelMA/HAMA patches were immersed in 10 mL MES buffer at pH 6. EDC and NHS were added successively, and samples were activated for 15 min at 37 °C. Then QHREDGS peptide was added in concentration 100 mg and reacted for 12 h at 37 °C. After the reaction, the patches were washed three times and freeze-dried for 48 h. FITC-labeled peptide was used to compare physically absorbed and chemically coupled peptides. For the physical condition, lyophilized patches were immersed in 10 mg mL^{-1} FITC-peptide solution for 12 h, washed three times, and freeze-dried. For the chemical condition, FITC-peptide was processed in the same manner as QHREDGS peptide. Thin and thick-filament patches were then immersed in 100 mL PBS solution for 37 °C with stirring at 100 rpm. Fluorescence was estimated on days 0, 3, 6, 9, 12, and 15. Relative fluorescence intensity was normalized to the initial value.

Human dermal fibroblasts and human umbilical vein endothelial cells were cultivated in DMEM/F12 medium supplemented with 10% fetal bovine serum and 1% antibiotic-antimycotic solution at 37 °C with 5% CO_2. Cells were assigned to control group (PBS), GelMA/HAMA patch extract, QHREDGS solution, and QHREDGS-coupled GelMA/HAMA patch extract groups. The treatment was performed for 48 h. Concentration of the soluble QHREDGS was selected to match the amount found in soaking solutions of peptide-coupled patches after 48 h.

Fibroblast cytocompatibility was estimated by means of Calcein-AM/PI staining and CCK-8 test. Cells were stained with 2 μL mL^{-1} Calcein-AM and 4 μL mL^{-1} propidium iodide for 1 h, washed with PBS, and photographed by means of fluorescence microscopy. Percentage of alive cells was calculated as a ratio of alive cells to total cells. To perform CCK-8 test, cells were incubated for 2 h with 10 μL of CCK-8 solution. Absorbance was measured at 450 nm. Cell viability was calculated as

$$\text{Cell viability}(\%) = \frac{\text{OD}_{\text{treatment}}}{\text{OD}_{\text{control}}} \times 100. \tag{2}$$

In this process, the control group culture without any treatment is considered as the baseline metabolic state. Values near 100% thus suggest that there was no inhibition of the metabolic rate of the fibroblasts when exposed to these exposure conditions due to the material extract and coupling process.

Fibroblast migration was determined through the scratch test method. HDF cells were first seeded on 6-well plates until confluent, after which a cell-free line was made using a 200 μL pipette tip, and cells were exposed for 48 hours. Images were captured at 0 and 48 hours, and migration was measured using ImageJ software. The migration ratio was determined as

$$\text{Migration ratio}(\%) = \frac{\text{initial scratch distance} - \text{scratch distance after growth}}{\text{initial scratch distance}} \times 100. \tag{3}$$

It shows the percentage of the original acellular gap filled with the cells after treatment. This does not provide a comprehensive understanding of the wound-healing process, but serves as a reasonable comparative measure for the migration of fibroblasts into a pre-established gap.

Endothelial organization was analyzed by a tube formation assay using growth factor-reduced Matrigel. The treated HUVECs were plated on Matrigel-coated plates at $\approx 6 \times 10^4$ cells mL^{-1} and cultured for 8 h. Tubular structures were visualized via light microscopy and their total length was quantified by ImageJ. Hemolysis was determined by co-incubation of 2% rat erythrocytes in PBS, GelMA/HAMA patches, QHREDGS solution, and QHREDGS-functionalized GelMA/HAMA patches for 5 h at 37 °C. Erythrocyte lysis was assessed by measuring the absorbance of the supernatants at 570 nm.

In the in vivo study, the male Sprague-Dawley rats were fasted overnight prior to the surgical procedure. The anesthesia was induced by i.p. administration of xylazine at 5 mg kg^{-1} and ketamine at 50 mg kg^{-1}. Full-thickness skin circular defects ($\approx$ 1.5 cm in diameter) were made on the back of the rats. The animals were equally divided into groups for PBS treatment, GelMA/HAMA patch application, QHREDGS solution and QHREDGS-functionalized GelMA/HAMA patch treatment, containing 5 rats each. The wounds were photographed at days 0, 3, 5, 7, and 9. The wound area was determined by ImageJ, and wound closure rate was calculated as

$$\text{Wound closure}(\%) = \frac{\text{initial wound area} - \text{residual wound area}}{\text{initial wound area}} \times 100. \tag{4}$$

The closure percentage was analyzed alongside histology, since area change alone does not differentiate between constructive tissue formation and contraction.

Sections of 5 μm were prepared from fixed, dehydrated, paraffin-embedded tissues and organs. Hematoxylin and eosin staining was done to analyze the regeneration of tissue and its compatibility. Masson's trichrome staining was performed to analyze the collagen

deposition. IL-6 and TNF-α immuno-histological analysis was done to analyze the inflammation level. The immunofluorescence analysis of CD31 and α-SMA was performed to analyze the vessels. Values are presented as mean $\pm$ SD. Statistical analysis was performed using GraphPad Prism software with one-way analysis of variance and Tukey's multiple-comparisons test. P¡0.05 was considered statistically significant.

Table 1: Assay conditions.

Parameter	**Condition or role**
Hydrogel formulation	15% GelMA, 5% HAMA, 1% HMPP, and 2% sodium alginate solution
Patch geometry	Printed circular lattice with approximately 15 mm diameter
Printing needles	20G for thick filaments of approximately 600 μm and 23G for thin filaments of approximately 300 μm
Crosslinking	365 nm ultraviolet light, 10 mW cm^{-2}, 5 min
Peptide immobilization	EDC/NHS coupling in MES buffer at pH 6, followed by 12 h reaction with QHREDGS at 37 °C
Degradation condition	2 U mL^{-1} collagenase II in PBS at 37 °C with daily enzyme replacement
Cellular readouts	HDF viability, HDF migration, HUVEC tube formation, and erythrocyte compatibility
Animal readouts	Wound closure, H&E morphology, IL-6, TNF-α, collagen deposition, CD31, and α-SMA

The assay conditions correlate each specific measurement with a biological or materials function. The GelMA/HAMA ink and photopolymerization determine lattice fabrication; the collagenase degradation assay determines the temporary network persistence; FITC labeling is used to quantify peptide residence time; and finally, the cell and animal assays investigate whether the presented QHREDGS alters the fibroblast, endothelial, inflammatory, collagen, and vascular response during repair.

3. Results and Discussion

3.1 Lattice architecture and enzymatic remodeling

The gelatin methacrylate/hyaluronic acid methacrylate (GelMA/HAMA) ink formed a circular lattice after extrusion and photopolymerization. The composition of 15% GelMA and 5% HAMA provided proper material continuity to retain the filament identity while having a hydrated composition adequate for soft tissue contacts. The optical morphology confirmed regular square openings throughout the patch area and blue-tinted continuous filaments without sheet collapse. Maintaining hydrogel architecture after deposition is a critical aspect of biological 3D-printing [36]. At higher magnification, the filaments had well-defined edges and contact points, which means that the 30 °C nozzle temperature and 10 °C printing bed temperature were enough to stabilize the deposition before ultraviolet curing. This result is critical because the patch must function as a porous interface, not as a blocking plug. It is also an example of the general additive manufacturing concept, according to which architecture can be controlled purposefully to match tissue function [37].

The lattice architecture and degradation pattern shown in Figure 2 represent two interrelated material characteristics. The printed lattice creates large channels between filaments on the millimeter-to-submillimeter scale, while SEM picture demonstrates sponge-like architecture with small pores. Additionally, the panel shows the collagenase II degradation, which resulted in progressive degradation up to about 51.4% by the end of day 7. The combination is beneficial for a wound patch, as the large channels allow wound fluid exchange and creation of non-dense interface, while small pores help to maintain hydration and enzymatic degradation. However, both large openings and pores create additional diffusion ways for unbound peptides, and thus ligand anchoring becomes crucial in the design.

Collagenase II degradation subjected the 3D-printed lattice to enzymatic stress. After seven days of incubation with 2 U mL^{-1} collagenase II, the patches degrade by about 51.4%. The result represents an intermediate level of degradation. The lattice is not so stable that it could be used as a long-term foreign interface, but it is also not so unstable that it disappears after exposure to proteolytic environment. For the full-thickness wound, such behavior is preferable since the first week is the period of inflammation, early fibroblast migration, endothelial sprouting, and granulation tissue formation. Thus, the patch could present ligands and maintain hydrated scaffold-like interface and yield space for collagen deposition.

The degradation result further explains the function of the GelMA/HAMA mixture. GelMA provides protein content sensitive to enzymes and interaction motifs, while HAMA adds hydration and glycosaminoglycan-like properties typical of hydrated soft-tissue environment. The mixture is more than just mixing two polymers for diversity of composition. It creates a network capable of being photocrosslinked into a printable form that is still subject to remodelling. It is essential for the biological interpretation of the results: better wound healing is not due to a permanently solid mechanical barrier since there was significant mass loss caused by the enzymes throughout the experiment period.

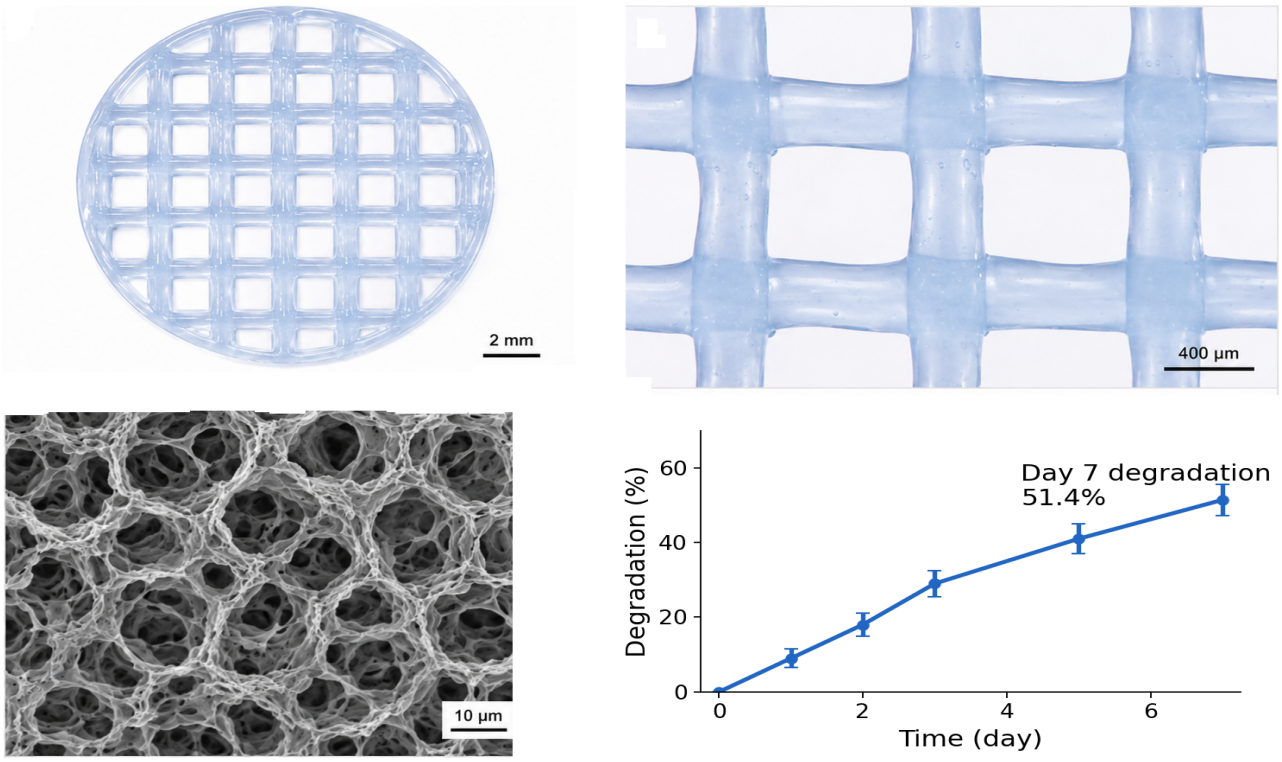

Figure 2: Architecture and enzymatic degradation.

3.2 Peptide presentation through anchored peptide in an open hydrogel network

Peptide retention was crucial for testing the material properties since it highlighted the defect created by open structure. At first, FITC-labeled peptide adsorbed on the gel structure was easily visible but its fluorescence diminished quickly during incubation. The highest decrease was observed in thin filament regions, which is explained by shorter distance to diffuse and increased surface-to-volume ratio. Thickening of the filaments helped to retain peptide somewhat, however, increasing the filament size is not optimal since it decreases printing resolution and makes less space open for interaction with the wound.

Table 2: Retention logic.

Peptide state	**Observed behavior**	**Interpretation**
Physical absorption in thin filaments	Fast fluorescence decline over the first days and minimal residual signal by day 15	Short diffusion pathways make fine printed structures vulnerable to burst loss of unbound peptide
Physical absorption in thick filaments	Slower loss than thin absorbed patches but continued major decline	Larger filaments reduce diffusion rate but do not provide stable peptide residence
Chemical coupling in thin filaments	Sustained fluorescence with much less early loss than absorbed thin patches	Covalent attachment protects peptide retention even in high-surface-area architecture
Chemical coupling in thick filaments	Highest retention among the tested conditions	Longer diffusion distance and covalent association act together to preserve peptide signal

As seen in Figure 3, the retention curves indicate that chemical coupling via EDC/NHS affected the release profile significantly. Coupled thin and thick films retained much more fluorescence after 15 days of degradation compared to physically absorbed thin films. In the coupled case, both retention curves stayed well above half of the initial signal until the last measurement point, while the physically absorbed films reached near-complete loss of fluorescence. This implies that the peptide residence in the films was no longer controlled by the passive diffusion out of hydrated pores. Residual fluorescence could reflect the association of peptides covalently bound to the degrading matrix.

It is crucial that the initial period is critical in the studied system. Between three and seven days, there is an establishment of inflammation signals, fibroblasts invasion, and activation of endothelial cells. If a burst of peptides was released before coordination of those events took place, it would provide only temporary effect. The coupled films retained enough fluorescence during the entire period, while physically absorbed groups lost a significant amount of it right from the start. It confirms covalent immobilization as an option to maintain bioactivity while keeping the printed open lattice. It agrees with results that demonstrate the increased microvascularization upon immobilization of angiogenic peptide while maintaining ligand accessibility [38].

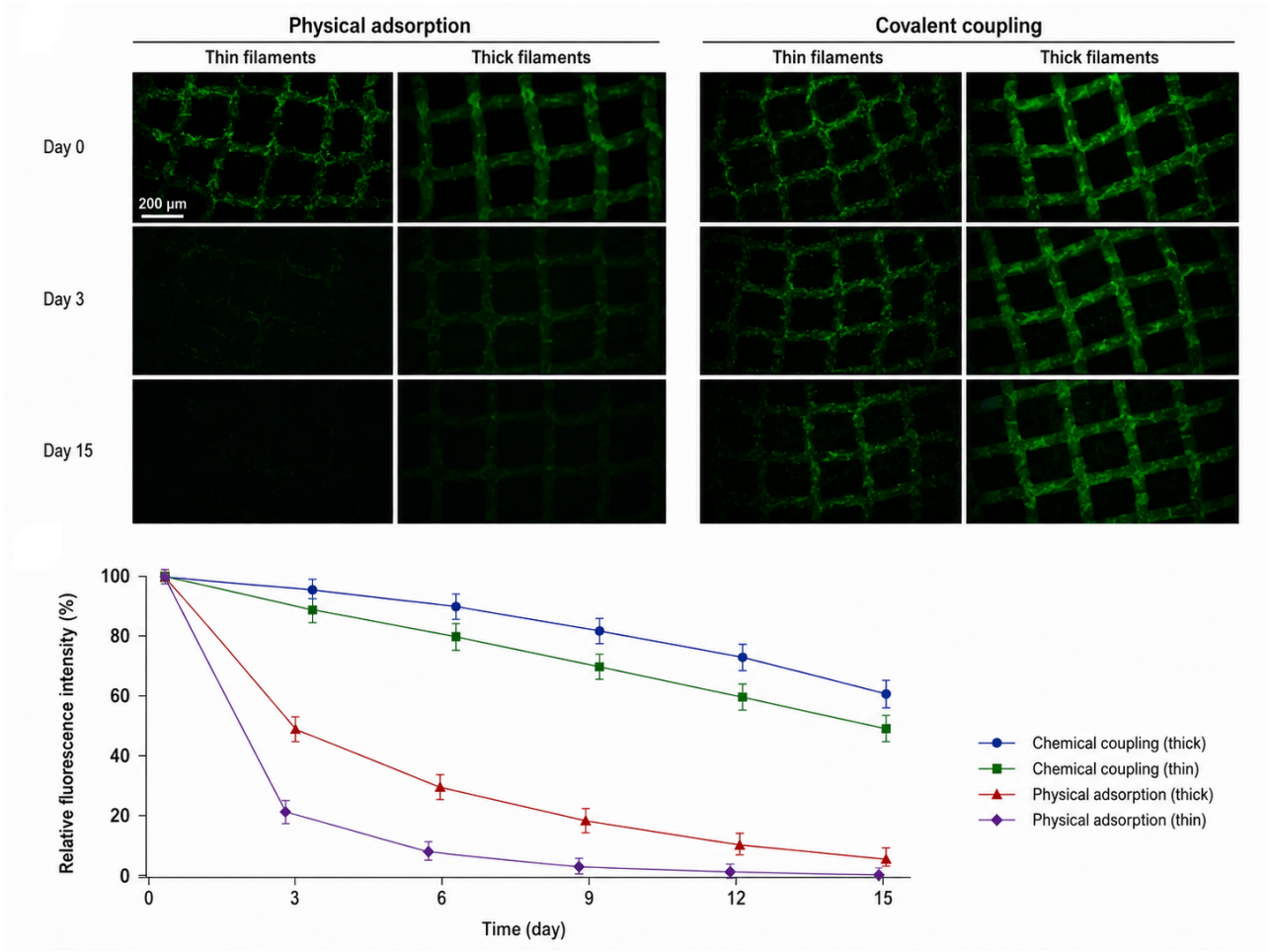

Figure 3: QHREDGS retention.

The contrast draws apart the effects on chemical vs. geometric loading. Physical loading is heavily dependent on filament diameter, whereas chemical loading mitigates the effect of having small filaments. This is because fine architecture is essential for both conformability and wound fluid access. A denser matrix could hinder diffusion, but it would defeat the purpose of printing a lattice. Using the coupled peptide would enable the material to take advantage of the benefits of a porous structure without premature degradation of the angiogenic signal.

3.3 Cytocompatibility and functional cell behavior

It is essential for a biofunctional hydrogel to be biocompatible in terms of its coupling protocol. Calcein-AM/PI staining revealed that most human dermal fibroblasts were green and alive, whereas few red cells were observed in all samples. No significant differences in cell density and morphology were observed among the PBS control, the patch extract, the QHREDGS solution, and the coupled patch extract. The quantitative measurements of live-cell analysis revealed consistent values around the middle-upper 90% range. According to the CCK-8 assays, there was no decrease in metabolism caused by either the patch extract or the coupled patch extract.

The proof of cytocompatibility in Figure 4 is an obligatory test in order to interpret later bioactivity. The live/dead staining reveals that in all control, patch, peptide, and coupled-patch samples, the predominant population consists of live fibroblasts, and the live-cell values are not different from the untreated culture. Additionally, the hemolysis assay introduces the screen for the material interaction with the blood: the patch, peptide, and coupled-patch samples are still far from the positive control and below 5% threshold shown in the plot. In the absence of these results, any increased cell migration or accelerated in vivo repair could have been explained by post-selection of cells and toxicity. In the absence of a cytotoxic effect and hemolytic effect, the washing procedure after coupling and photo polymerization of GelMA/HAMA network can be considered biocompatible.

The scratch assay revealed that the presence of QHREDGS changes fibroblast behavior. Limited scratch healing was seen after 48 hours for PBS and patch extract; however, a significantly higher amount of migration was observed for the solutions of peptide and the peptide-coupled patch extract. The approximate migration ratio grew from the low range of 15-20% in the control and patch-only sample groups to approximately 70% in the solution of QHREDGS and mid-80% range in the coupled-patch group. This hierarchy reveals that QHREDGS peptide is responsible for fibroblast migration and that coupling did not affect its biological activity. Migration is important due to the contribution of the dermal fibroblast into the granulation tissue formation, wound contraction, and collagen deposition, so scratch healing can serve as a connection between the material design and wound healing outcome.

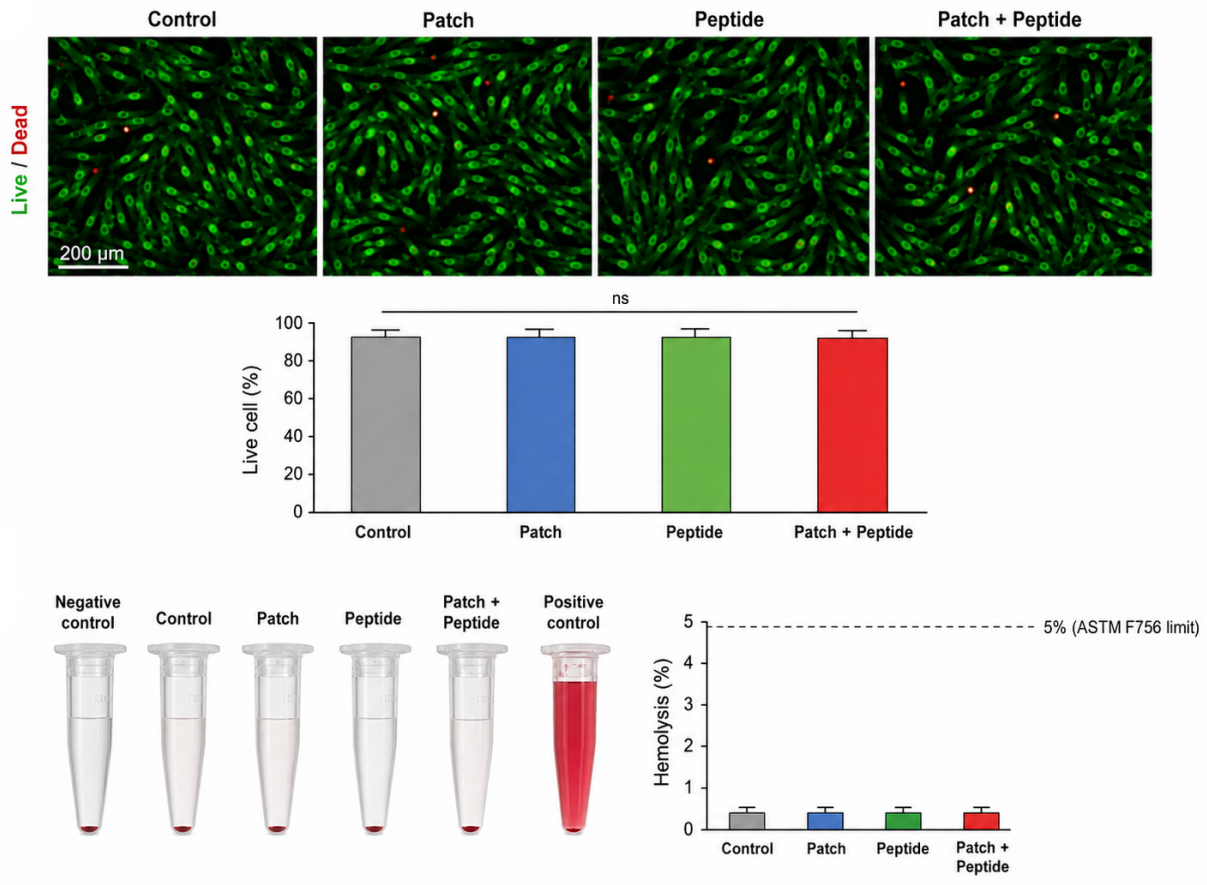

Figure 4: Cytocompatibility and hemolysis.

The pair of migration and tube formation assays in Figure 5 provides the connection between the response of dermal and endothelial cells in a single test. The scratch panels show more rapid coverage of the scratched area with fibroblasts in the presence of QHREDGS peptide. At the same time, HUVEC tube formation is more prominent in the QHREDGS solution and patch-plus-peptide sample than in the controls.

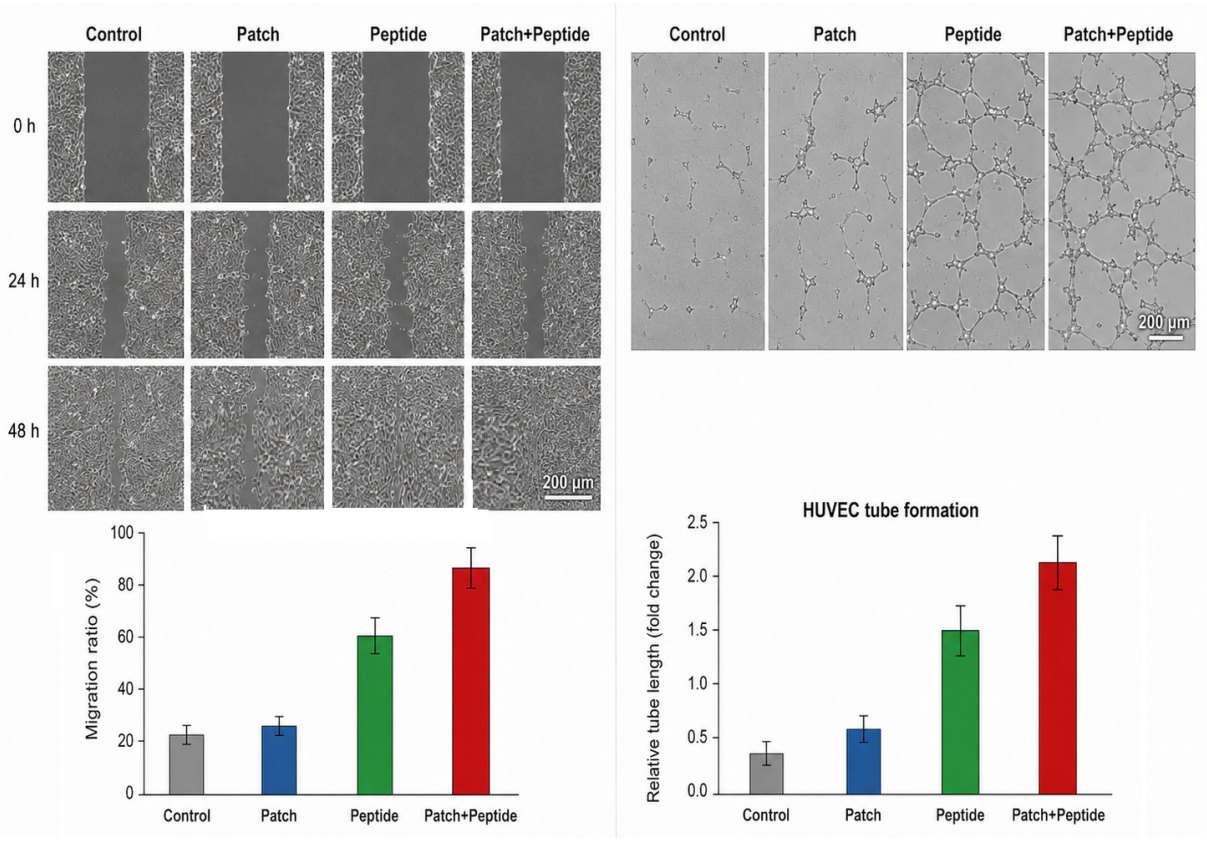

Figure 5: Migration and tube formation.

HUVEC tube formation is weak in the case of PBS and patch-only sample, and it increases significantly in QHREDGS solution and patch-plus-peptide conditions. Patch-plus-peptide condition reveals the highest tube formation, which is approximately four to five times higher compared to the control by visual inspection of bar plots. This paired behavior is biologically relevant, as the regeneration of skin wounds involves the coordination of fibroblasts and endothelial cells. The role of fibroblasts includes collagen deposition and remodeling, while endothelial cells organization provides vascularization and necessary delivery of nutrients and oxygen.

The combined findings on viability, migration, and tube formation further differentiate carrier role from signaling role. The gel matrix acts as a permissive carrier that is compatible with fibroblasts and can be constructed as a porous scaffold. However, it is not a primary inducer of migration or angiogenic organization. Soluble QHREDGS peptide is a proof of the bioactivity of the amino acid chain; however, this soluble form lacks a material mechanism for localization of the signal. The combined patch uses the strength of both mechanisms: cytocompatible degradable scaffold and localized angiogenic ligand.

3.4 Full thickness wound closure and tissue reconstruction

Rat full thickness wound model was used in order to test if the obtained material-cell relationship results in effective repair at the tissue level. Closure increased from day 0 to day 9 as it should be in an acute wound model. Rates and extents of closures were quite different among the treatment groups. PBS control group and GelMA/HAMA patches resulted in reduced closure rates. Soluble QHREDGS helped to improve the outcome but coupled patch performed the best and resulted in the highest degree of closure and minimal wound area at day 9. According to the quantified plot, closure at day 9 was approximately two thirds of the original size in the control group, around three fourths in the patches-only group, almost 90% in soluble peptide group and almost complete in the coupled patch group.

Images series and closure profiles in Fig. 6 follow the order determined in the retention and cell studies. Patches-only produce hydrated printed interface but their closure response is similar to that of controls. Soluble peptide resulted in clear biological benefit and shows that QHREDGS can stimulate wound healing in presence. The coupled patch performed best due to localized peptide signal in degradable wound contact material. The results indicate that peptide immobilization is necessary in order to turn a structure-wise correct hydrogel into a material stimulating healing. If it was sufficient to use the coverage, the patch-only group would perform almost as good as the coupled patch group.

Macroscopic closure alone is often deceptive if one does not have histological information. Therefore, hematoxylin and eosin staining provided a complementary endpoint. Groups with peptides contained thicker regenerated tissues than groups with PBS and patches only, and coupled patch group resulted in the highest degree of development of the tissue response. This result means that there is not only improvement in wound closure but in tissue reconstruction as well. This is consistent with in vitro findings since better migration and organization of endothelium are expected to provide a better granulation bed.

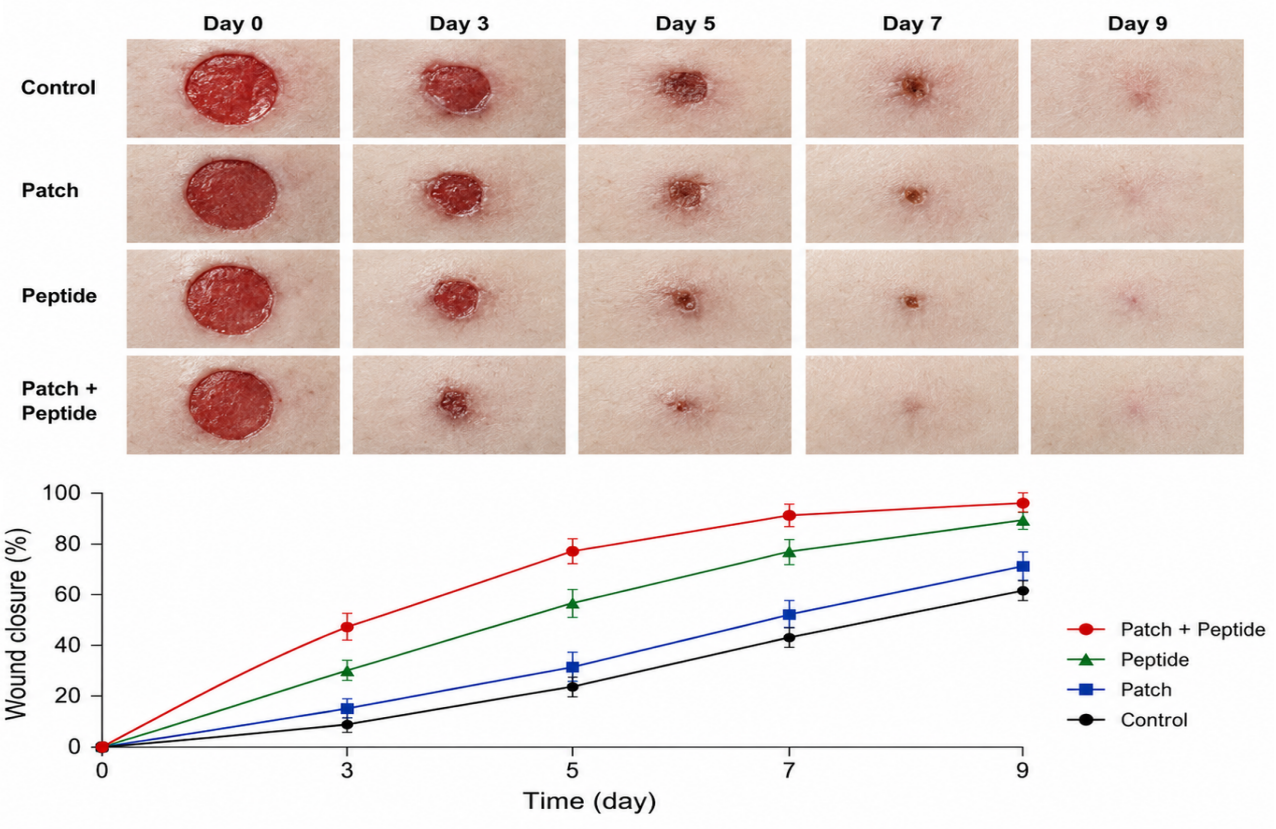

Figure 6: In vivo wound closure.

In the panels of histological staining and collagen labeling in Fig. 7, we can observe that the reduction in area response is associated with an increased tissue bed. The H&E stained sections change from a less thick and less complete regenerate tissue in the control group to a more thick and complete regenerating region in the coupled patch group. Similarly, in the case of Masson's trichrome staining, the group showing the largest positive collagen region is the patch plus peptide group.

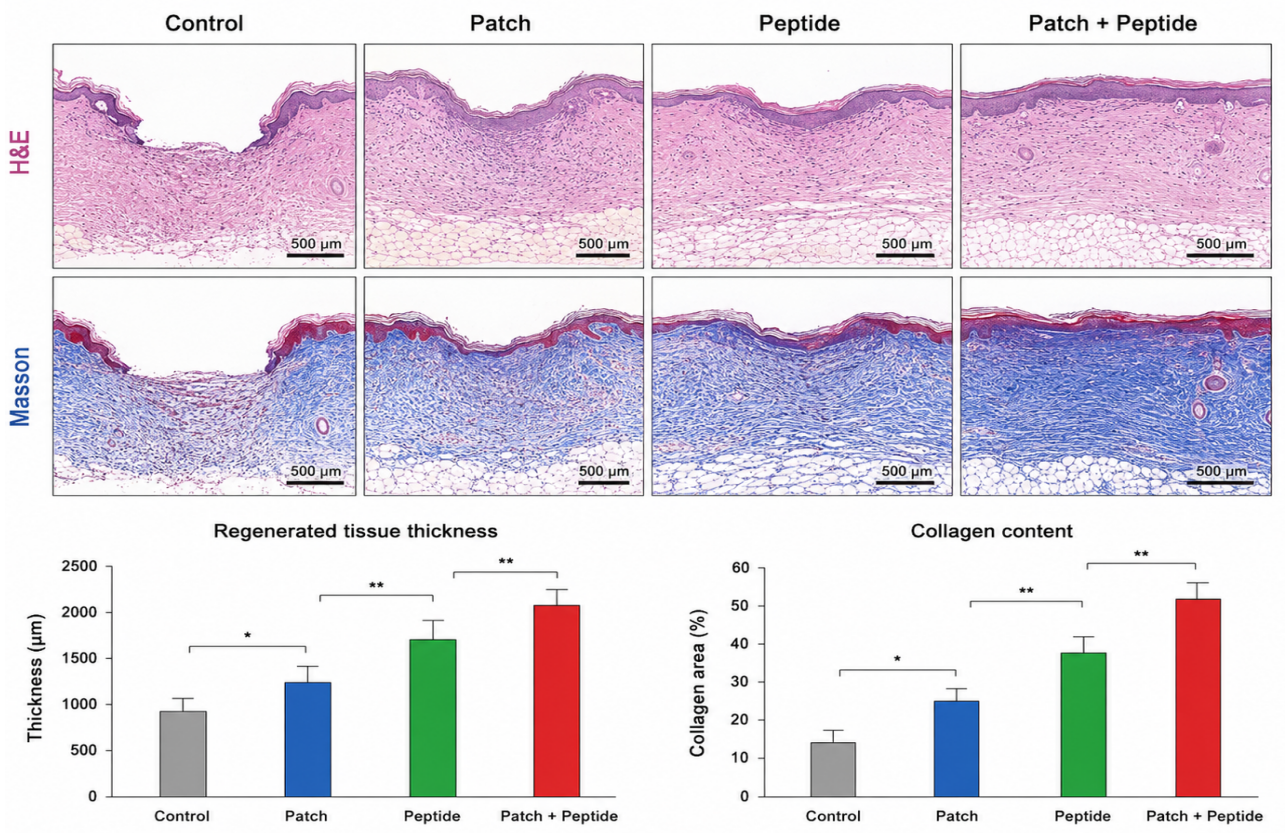

Figure 7: Histology and collagen deposition.

The significance of the timing of the experiment is worth noting as well. Since day 9, acute rat wounds have not yet matured into scarring; thus, the differences in the wound closure, collagen deposition, inflammation, and vascularization show a result of initial healing rather than the final outcome. According to the experiment, the patch with the peptides appears to facilitate the transition from the stage of inflammation-induced injury to the stage of formation of collagen and vascularized tissue. Even though the results do not confirm the scar-free healing of the wound and the restoration of the hair follicle tissue, they still show that the material is capable of affecting the trajectory of the healing process positively.

3.5 Inflammation, collagen deposition, and vascular maturation

Histological analysis of inflammatory markers showed a tissue-level evaluation of how the material affected the inflammatory signaling in wounds. As it is shown on Figures 7(a,b), IL-6 and TNF-α expression was maximal in PBS controls and high in the case of the GelMA/HAMA patch group. Application of the QHREDGS solution lowered the levels of these markers and the patch with the peptides lowered them even more. Quantified staining bars show that IL-6 levels were reduced from approximately 2.7 to 0.6 folds, while TNF-α levels were reduced from approximately 2.4 to 0.5 folds. This is biologically significant since hydrogel-mediated regulation of excessive inflammatory signaling promotes wound healing [39].

In contrast to inflammatory markers, the collagen deposition in the Figure 7(c,d) increased in the opposite direction. Collagen content was minimal in PBS controls, moderately higher in the GelMA/HAMA patch group, considerably higher in the group with soluble QHREDGS, and maximal in the coupled-patch group. In particular, in the coupled-patch group, collagen content increased approximately to 2.2 folds according to the quantified bar graphs. The reciprocal trend is essential since the inhibition of excessive inflammation and collagen deposition indicate the shift of wound healing towards the stage of tissue replacement. In other words, the patch had to both inhibit inflammation and increase collagen deposition, which is what was observed in the coupled group.

The interaction between the rate of degradation and collagen deposition has to be discussed separately. According to Figure **??**(a,b), the hydrogel degraded by approximately 51.4% within seven days in collagenase II. At the same time, the collagen deposition was maximal in the coupled-patch group in nine days. Thus, these results show the process of wound healing through tissue replacement rather than just masking the injury with a hydrogel layer. Namely, it shows that the scaffold has to be replaced by the collagenous wound tissue, which corresponds to the principle of regenerative hydrogels [31].

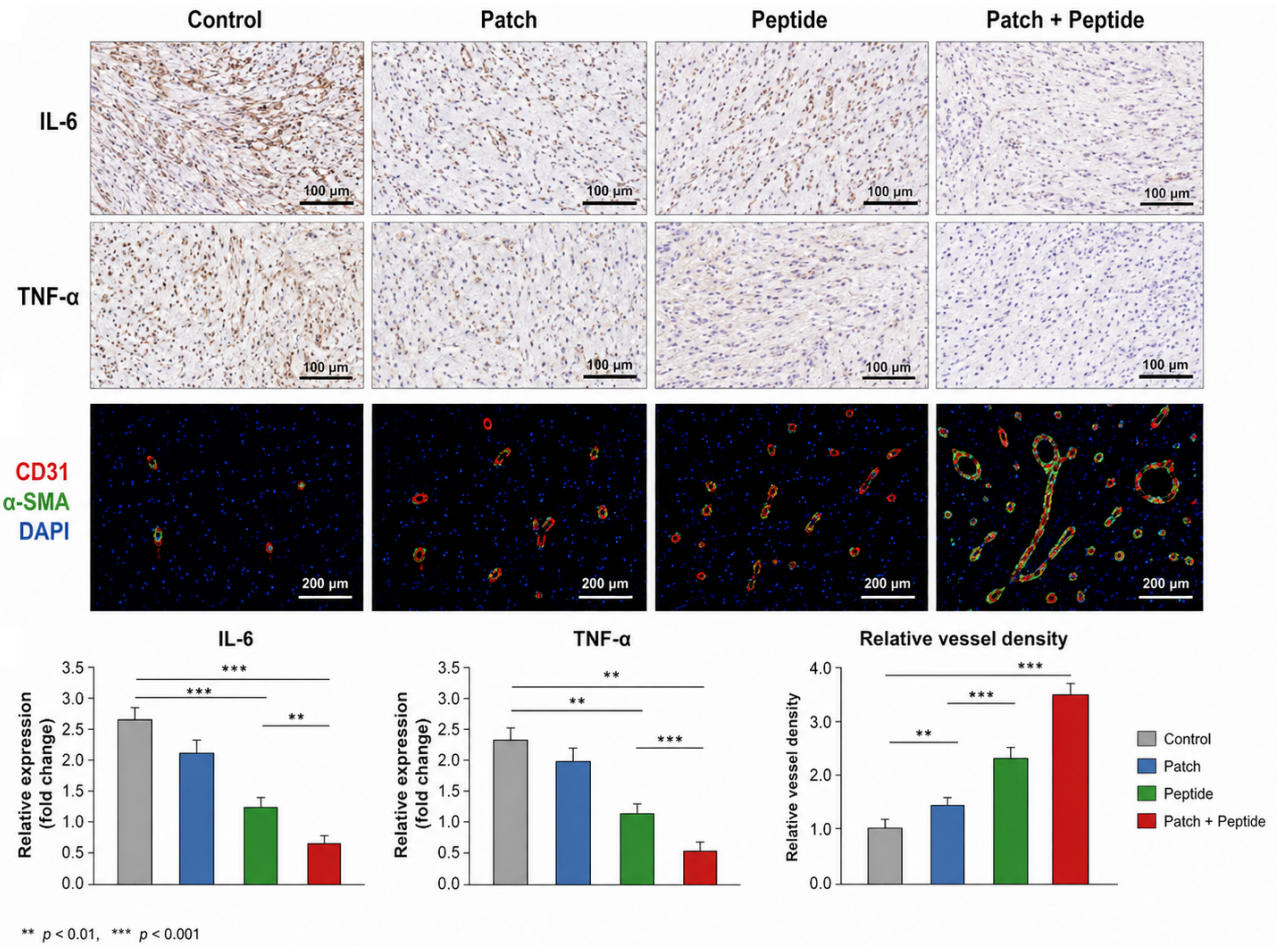

Figure 8: Inflammation and vascularization.

The neovascularization was characterized through immunofluorescence analysis for CD31 and α-SMA. CD31 stains the endothelium, while α-SMA stains smooth muscle-like/perivascular structures indicating stabilization of vessels. Staining was limited in control wounds and showed only minor improvement with the use of the patch alone. Soluble QHREDGS increased vessel staining, and the coupling of the patch with the peptide resulted in the best staining of the vessel system. Relative vessel density increased from about 1.0 in the controls to about 3.7 in the coupled patch group. These inflammatory and vascular data are shown collectively in Figure 8.

Of all the results presented in Figure 8, the one that best explains the better outcomes in terms of closure and collagen is the inflammatory and vascular staining. Having endothelial cells involved is good enough, but the appearance of α-SMA-positive cells indicates a greater organization in the vascular response compared to only endothelial sprouting. This is supported by the role of angiopoietin, which stabilizes vessels and maintains the survival of endothelial cells [17]. The organization of vasculature would facilitate the activities of fibroblasts, oxygen supply, and formation of collagen-rich tissues as well as alleviate chronic inflammation. It seems that the coupled patch improves wound healing via improving the vascular-collagen feedback loop through better retention of QHREDGS.

As seen from the comparative analysis profile, the patch containing the peptide did not work via just one endpoint. The positive effect was obtained throughout the entire repair pathway – from fibroblast adhesion, through cell migration, re-organization of the blood vessels, closure, regeneration of tissues, inflammation decrease, collagen deposition, and development of the mature vasculature. Patch without the peptide is the control test proving that the GelMA/HAMA matrix can serve as the cytocompatible carrier. Soluble peptide is another control test which proves the bioactivity of QHREDGS. Coupling of the peptide with the matrix allows combining the degradation process of the printed structure and the biochemical presentation of the growth factor.

One additional point should be made when analyzing the plotted data in regard to time. While the retention experiment shows that the amount of the absorbed peptides starts separating from the material early, the animal wound study shows the maximum gap between different treatments at the early to middle stage of the repair period. This connection supports the suggestion that peptide residence in a material is not just the cosmetic characteristic but an important part of the tissue function. Coupled patch does not have to deliver a strong burst of the growth factor into the wound fluids. It can provide the local ligand-rich interface which will allow cells to remodel the local hydrogel.

The patch-only group allows us not to exaggerate the therapeutic potential of the polymer blend itself. GelMA/HAMA is printable, hydrophilic, porous and cytocompatible. However, those are just the basic characteristics of the permissive carrier. The biological shift can happen only due to the presence of QHREDGS. However, on the other hand, the soluble peptide group allows us not to consider

the gel matrix as just a passive container. While QHREDGS itself is bioactive, the difference between soluble and coupled patches shows that the method of presentation is important. As a wound surface is constantly diluted by exudate and remodeled by proteases, local retention of the peptide can turn a transient molecule into a long-term interface signal. The treatment regime shows the separation of roles: GelMA/HAMA controls the form and the degradation process, QHREDGS controls the instructions for cell migration and angiogenesis and covalent coupling connects these functions.

Table 3: Integrated repair profile.

Endpoint	**PBS**	**GelMA/HAMA**	**QHREDGS**	**Coupled patch**
Fibroblast viability	Calcein-positive cells dominate; CCK-8 near control	Calcein-positive cells dominate; no extract toxicity	Calcein-positive cells dominate	Calcein-positive cells dominate after coupling
Fibroblast migration	About 15–20% scratch occupation	About 15–20% scratch occupation	Approximately 70% scratch occupation	Mid-80% scratch occupation
Endothelial tubes	Sparse tube network	Sparse tube network	Marked tube extension	About 4–5-fold tube-length increase relative to control
Day-9 closure	About two-thirds closure	Roughly three-quarters closure	Around 90% closure	Nearly complete closure
H&E tissue repair	Thin regenerated tissue	Limited thickening	Thicker granulation tissue	Most developed regenerated tissue
IL-6/TNF-α	About 2.7/2.4-fold staining	Elevated staining	Lower staining than controls	About 0.6/0.5-fold staining
Collagen deposition	Weak trichrome signal	Modest trichrome signal	Increased trichrome signal	Approximately 2.2-fold collagen content
CD31/α-SMA	Relative vessel density near 1.0	Slight vascular increase	Increased vascular staining	Relative vessel density near 3.7

Collagen and vascular staining results suggest that the material had an impact on the quality of repair process, not on the closure speed. Contraction is the reason of the rapid closure in rodents, and it could overestimate the regenerative capacity. The combination of thicker tissue layer, increased collagen level and number of CD31/α-SMA-positive structures implies that the reduction of the area was achieved by biological reconstruction of the tissue. The drop of IL-6 and TNF-α levels suggests that the wound environment did not stay in the inflammatory phase. These two results are interconnected. The better vascular bed can allow survival and collagen synthesis by fibroblasts; the organized collagen can help to stabilize the vessels, and the decreased inflammatory load can minimize the destruction of the newly formed tissue.

3.6 Coordinated peptide retention and repair mechanism

Material contribution involves a well-known dilemma in regenerative hydrogels: transport-enhancing features reduce peptide residence; residence-enhancing features retard remodeling. The findings solve the dilemma in a single construct: the printed lattice stays open; the GelMA/HAMA network stays degradable; QHREDGS remains localized within the hydrogel. The conclusion is not based on an overall hypothesis about the benefit of three-dimensional printing in wound healing or the utility of angiogenic peptides. The findings are supported by the simultaneous existence of open architecture, enzyme degradation, and ligand immobilization in a wound-contacting patch.

The result chain is consistent. Morphology and collagenase degradation define the patch as a temporary porous interface; FITC staining demonstrates that physical adsorption and chemical immobilization create different peptide residence profiles; fibroblast and endothelial assays confirm that immobilization does not prevent the activity of QHREDGS. The animal outcomes then indicate that local delivery is associated with rapid closure, reduced inflammatory staining, improved collagen deposition, and increased CD31/α-SMA-positive vessel density. Therefore, chemical binding of QHREDGS is the material innovation that transforms a printable GelMA/HAMA lattice into a bioactive wound interface.

The evidence favors a mechanistic explanation in which peptide residence is the key factor. The printed lattice offers the required geometry for wound contact and fluid exchange, but its open structure creates a risk of rapid peptide loss. The EDC/NHS coupling addresses this problem by immobilizing QHREDGS within the hydrogel matrix. In turn, the degradation prevents the material from functioning permanently; immobilization retains the peptide active long enough to affect fibroblasts and endothelium. Thus, the chain explains why the coupled patch outperforms the hydrogel and the soluble peptide. The hydrogel provides the required structure, but it lacks biological instructions. The soluble peptide provides biological instructions, but it cannot retain them locally. The coupled patch provides both.

The datasets describe a repair process rather than a stand-alone outcome. The treatment that heals the wounds most quickly also enhances the prior stages that provide a basis for rapid healing: peptide residence, cell compatibility, migration, tube formation, reduction of inflammation, collagen deposition, and vessel density. The retention assay would have been incomplete if immobilization

had deactivated QHREDGS; in vitro assays would have been incomplete if animal wounds had failed to heal; and wound closure outcomes would have been incomplete if histological examination had revealed low collagen deposition and persistent inflammation. The coupled-patch group is convincing because the material and biological outcomes agree.

The evidence clarifies the effect of QHREDGS in a way that is applicable to peptide-based materials in general. Peptides can be used as soluble factors, but many signaling molecules of tissue engineering act via local contact, adhesion-related mechanisms, or network-based ligand presentation. Covalent immobilization can maintain the local signal while minimizing burst release, as long as the ligand stays accessible and the coupling procedure does not deactivate it. The data presented here suggest that QHREDGS remains functionally active after immobilization because both fibroblast migration and endothelial tube formation increased. The result is consistent with earlier studies, which demonstrated that the ligand presentation in a GelMA context affects the vascular response [38].

The four experimental groups separate the contributions of individual components. PBS represents the control wound condition; the GelMA/HAMA patch checks the printed matrix; soluble QHREDGS checks the ligand; and the coupled patch checks the combination of carrier and ligand. This separation allows to identify whether the observed benefits are due to the hydrogel, the peptide, or their combination. The thin-filament and thick-filament retention assay improves the materials analysis because it shows that immobilization works in different diffusion distances.

Several limitations still exist. The animal experiment lasted nine days, which is sufficient for early wound closure and granulation, but not for full scar development, appendage regeneration, and tensile properties; mechanical properties were not tested before and after collagenase exposure, although swelling, compression, adhesion, and softening of the patch during enzymatic decomposition can influence its retention on the moving skin. FITC fluorescence provided a clear comparative retention profile, but it did not allow to assess coupling efficiency, ligand density, and accessible ligand fraction; and the wound model was limited to acute clean wound; diabetic, ischemic, infected or very exudative wounds would have created additional challenges in terms of inflammation, enzymes, and microbes. These limitations do not invalidate the primary conclusion, but they set directions for future research.

In future work it will be necessary to assess coupling efficiency, ligand density, and bioaccessible peptide fraction; measure the mechanical evolution of the patch during collagenase exposure; compare filament distance and layer thickness; and conduct extended wound-healing experiments that would involve scar maturation. Dose-response studies will be especially important, since high immobilized peptide density might not necessarily be beneficial if ligand overcrowding disrupts cellular adhesion and migration. More challenging wounds would help to establish whether QHREDGS presentation can enhance impaired angiogenesis in diabetic or ischemic conditions.

4. Conclusion

First, does the covalent QHREDGS anchoring enable a printed GelMA/HAMA lattice to maintain an angiogenic peptide signal while degrading enough to permit full-thickness wound healing? The acute wound experiments have confirmed a positive answer to this question. A 15% GelMA and 5% HAMA ink mixed with 1% HMPP and 2% sodium alginate could form circles of about 15 mm in diameter through printing, and UV curing made it stable in shape. Optical and SEM data confirmed that this is an open lattice of sponge-like internal structure. The exposure to collagenase II led to approximately 51.4% degradation of the patch in seven days. Thus, the patch is a temporary remodelable scaffold rather than a permanent barrier.

The crucial material feature is the difference between physical adsorption and covalent coupling. While physically adsorbed FITC-peptide was rapidly washed out, especially from thin filaments, showing the effect of the diffusion penalty for unbound molecules created by the open architecture of the printed lattice, covalent coupling ensured the presence of the strong fluorescent signal even after 15 days. Moreover, in this geometry, which is the most susceptible to peptide loss, the signal remained biologically active. Extracts from the patches containing peptide were cytocompatible to human dermal fibroblasts, QHREDGS-containing materials enhanced migration of fibroblasts, and endothelial tube formation was highest for the patch coupled to the peptide.

Thus, the important practical conclusion is that printed wound patches should be engineered based on the residence time of their active cue as well as the identity of the polymer. In this case, the anchoring of the peptide made possible for an open printed structure to avoid the problem of the burst loss typical for the porous hydrogels. As the same patch was able to degrade when exposed to collagenase, the construct remained compatible with the replacement of the provisional material by the native dermal tissues. Therefore, in the studied conditions, this material system has a clear biological role, being a remodelable carrier with its biological function supported by covalent ligand presentation at the wound-facing interface.

The animal experiments confirmed the connection between peptide residence and tissue regeneration. Thus, the GelMA/HAMA patch with covalently anchored QHREDGS demonstrated the fastest wound closure, the development of the most advanced regenerated tissue, the lowest level of IL-6 and TNF-α staining, the highest collagen deposition, and the most pronounced neovascularization marked by CD31/α-SMA-positive cells. All these features show that the patch is not just a hydrated cover but provides its biological function through the integration of the following abilities: the ability to ensure contact with the wound due to the print-defined porosity, degradation to allow the replacement of the patch by the tissue, and covalent presentation of the QHREDGS peptide to instruct

angiogenesis.

References

[1] Singer, A. J., & Clark, R. A. (1999). Cutaneous wound healing. New England journal of medicine, 341(10), 738-746.
[2] Gurtner, G. C., Werner, S., Barrandon, Y., & Longaker, M. T. (2008). Wound repair and regeneration. Nature, 453(7193), 314-321.
[3] Landén, N. X., Li, D., & Ståhle, M. (2016). Transition from inflammation to proliferation: a critical step during wound healing. Cellular and Molecular Life Sciences, 73(20), 3861-3885.
[4] Eming, S. A., Martin, P., & Tomic-Canic, M. (2014). Wound repair and regeneration: mechanisms, signaling, and translation. Science translational medicine, 6(265), 265sr6-265sr6.
[5] Boateng, J. S., Matthews, K. H., Stevens, H. N., & Eccleston, G. M. (2008). Wound healing dressings and drug delivery systems: a review. Journal of pharmaceutical sciences, 97(8), 2892-2923.
[6] Guo, S. A., & DiPietro, L. A. (2010). Factors affecting wound healing. Journal of dental research, 89(3), 219-229.
[7] Zhao, R., Liang, H., Clarke, E., Jackson, C., & Xue, M. (2016). Inflammation in chronic wounds. International journal of molecular sciences, 17(12), 2085.
[8] Caló, E., & Khutoryanskiy, V. V. (2015). Biomedical applications of hydrogels: A review of patents and commercial products. European polymer journal, 65, 252-267.
[9] Van Den Bulcke, A. I., Bogdanov, B., De Rooze, N., Schacht, E. H., Cornelissen, M., & Berghmans, H. (2000). Structural and rheological properties of methacrylamide modified gelatin hydrogels. Biomacromolecules, 1(1), 31-38.
[10] Nichol, J. W., Koshy, S. T., Bae, H., Hwang, C. M., Yamanlar, S., & Khademhosseini, A. (2010). Cell-laden microengineered gelatin methacrylate hydrogels. Biomaterials, 31(21), 5536-5544.
[11] Yue, K., Trujillo-de Santiago, G., Alvarez, M. M., Tamayol, A., Annabi, N., & Khademhosseini, A. (2015). Synthesis, properties, and biomedical applications of gelatin methacryloyl (GelMA) hydrogels. Biomaterials, 73, 254-271.
[12] Highley, C. B., Prestwich, G. D., & Burdick, J. A. (2016). Recent advances in hyaluronic acid hydrogels for biomedical applications. Current opinion in biotechnology, 40, 35-40.
[13] Velasco-Rodriguez, B., Diaz-Vidal, T., Rosales-Rivera, L. C., García-González, C. A., Alvarez-Lorenzo, C., Al-Modlej, A., ... & Taboada, P. (2021). Hybrid methacrylated gelatin and hyaluronic acid hydrogel scaffolds. Preparation and systematic characterization for prospective tissue engineering applications. International Journal of Molecular Sciences, 22(13), 6758.
[14] Murphy, S. V., & Atala, A. (2014). 3D bioprinting of tissues and organs. Nature biotechnology, 32(8), 773-785.
[15] Smandri, A., Nordin, A., Hwei, N. M., Chin, K. Y., Abd Aziz, I., & Fauzi, M. B. (2020). Natural 3D-printed bioinks for skin regeneration and wound healing: A systematic review. Polymers, 12(8), 1782.
[16] Potente, M., Gerhardt, H., & Carmeliet, P. (2011). Basic and therapeutic aspects of angiogenesis. Cell, 146(6), 873-887.
[17] Rouwkema, J., & Khademhosseini, A. (2016). Vascularization and angiogenesis in tissue engineering: beyond creating static networks. Trends in biotechnology, 34(9), 733-745.
[18] Briquez, P. S., Clegg, L. E., Martino, M. M., Gabhann, F. M., & Hubbell, J. A. (2016). Design principles for therapeutic angiogenic materials. Nature Reviews Materials, 1(1), 15006.
[19] Phelps, E. A., Landázuri, N., Thulé, P. M., Taylor, W. R., & García, A. J. (2010). Bioartificial matrices for therapeutic vascularization. Proceedings of the National Academy of Sciences, 107(8), 3323-3328.
[20] Hajimiri, M., Shahverdi, S., Kamalinia, G., & Dinarvand, R. (2015). Growth factor conjugation: strategies and applications. Journal of biomedical materials research Part A, 103(2), 819-838.
[21] Ahrens, V. M., Bellmann-Sickert, K., & Beck-Sickinger, A. G. (2012). Peptides and peptide conjugates: therapeutics on the upward path. Future medicinal chemistry, 4(12), 1567-1586.
[22] Erak, M., Bellmann-Sickert, K., Els-Heindl, S., & Beck-Sickinger, A. G. (2018). Peptide chemistry toolbox–Transforming natural peptides into peptide therapeutics. Bioorganic & medicinal chemistry, 26(10), 2759-2765.
[23] Miklas, J. W., Dallabrida, S. M., Reis, L. A., Ismail, N., Rupnick, M., & Radisic, M. (2013). QHREDGS enhances tube formation, metabolism and survival of endothelial cells in collagen-chitosan hydrogels. PLoS One, 8(8), e72956.
[24] Dang, L. T., Feric, N. T., Laschinger, C., Chang, W. Y., Zhang, B., Wood, G. A., ... & Radisic, M. (2014). Inhibition of apoptosis in human induced pluripotent stem cells during expansion in a defined culture using angiopoietin-1 derived peptide QHREDGS. Biomaterials, 35(27), 7786-7799.
[25] Martin, P. (1997). Wound healing–aiming for perfect skin regeneration. Science, 276(5309), 75-81.
[26] Werner, S., & Grose, R. (2003). Regulation of wound healing by growth factors and cytokines. Physiological reviews, 83(3), 835-870.
[27] MacNeil, S. (2007). Progress and opportunities for tissue-engineered skin. Nature, 445(7130), 874-880.
[28] Fife, C. E., & Carter, M. J. (2012). Wound Care Outcomes and Associated Cost Among Patients Treated in US Outpatient Wound Centers: Data From the US Wound Registry. Wounds: a compendium of clinical research and practice, 24(1), 10-17.
[29] Drury, J. L., & Mooney, D. J. (2003). Hydrogels for tissue engineering: scaffold design variables and applications. Biomaterials, 24(24), 4337-4351.
[30] Seliktar, D. (2012). Designing cell-compatible hydrogels for biomedical applications. Science, 336(6085), 1124-1128.
[31] Annabi, N., Nichol, J. W., Zhong, X., Ji, C., Koshy, S., Khademhosseini, A., & Dehghani, F. (2010). Controlling the porosity and microarchitecture of hydrogels for tissue engineering. Tissue Engineering Part B: Reviews, 16(4), 371-383.
[32] Tonnesen, M. G., Feng, X., & Clark, R. A. (2000, December). Angiogenesis in wound healing. In Journal of investigative dermatology symposium proceedings (Vol. 5, No. 1, pp. 40-46). Elsevier.
[33] Loessner, D., Meinert, C., Kaemmerer, E., Martine, L. C., Yue, K., Levett, P. A., ... & Hutmacher, D. W. (2016). Functionalization, preparation and use of cell-laden gelatin methacryloyl–based hydrogels as modular tissue culture platforms. Nature protocols, 11(4), 727-746.
[34] Mouser, V. H. M., Abbadessa, A., Levato, R., Hennink, W. E., Vermonden, T., Gawlitta, D., & Malda, J. (2017). Development of a thermosensitive HAMA-containing bio-ink for the fabrication of composite cartilage repair constructs. Biofabrication, 9(1), 015026.
[35] Hospodiuk, M., Dey, M., Sosnoski, D., & Ozbolat, I. T. (2017). The bioink: A comprehensive review on bioprintable materials. Biotechnology advances, 35(2), 217-239.
[36] Hinton, T. J., Jallerat, Q., Palchesko, R. N., Park, J. H., Grodzicki, M. S., Shue, H. J., ... & Feinberg, A. W. (2015). Three-dimensional printing of complex biological structures by freeform reversible embedding of suspended hydrogels. Science advances, 1(9), e1500758.
[37] Zadpoor, A. A., & Malda, J. (2017). Additive manufacturing of biomaterials, tissues, and organs. Annals of biomedical engineering, 45(1), 1-11.
[38] Parthiban, S. P., Rana, D., Jabbari, E., Benkirane-Jessel, N., & Ramalingam, M. (2017). Covalently immobilized VEGF-mimicking peptide with gelatin methacrylate enhances microvascularization of endothelial cells. Acta biomaterialia, 51, 330-340.
[39] Bian, J., Cai, F., Chen, H., Tang, Z., Xi, K., Tang, J., ... & Chen, L. (2021). Modulation of local overactive inflammation via injectable hydrogel microspheres. Nano Letters, 21(6), 2690-2698.